

PAPER • OPEN ACCESS

Unified equation of state for the outer and inner crusts of magnetars

To cite this article: Y D Mutafchieva *et al* 2020 *J. Phys.: Conf. Ser.* **1555** 012015

View the [article online](#) for updates and enhancements.

You may also like

- [Accurate and consistent automatic seismocardiogram annotation without concurrent ECG](#)
A Laurin, F Khosrow-Khavar, A P Blaber et al.
- [Dense Molecular Gas in the Nearby Low-metallicity Dwarf Starburst Galaxy IC 10](#)
Amanda A. Kepley, Lauren Bittle, Adam K. Leroy et al.
- [Uranus in Northern Midspring: Persistent Atmospheric Temperatures and Circulations Inferred from Thermal Imaging](#)
Michael T. Roman, Leigh N. Fletcher, Glenn S. Orton et al.



ECS
The
Electrochemical
Society
Advancing solid state &
electrochemical science & technology

DISCOVER
how sustainability
intersects with
electrochemistry & solid
state science research

Unified equation of state for the outer and inner crusts of magnetars

Y D Mutafchieva¹, Zh K Stoyanov¹, N Chamel², J M Pearson^{2,3} and L M Mihailov⁴

¹ Institute for Nuclear Research and Nuclear Energy, Bulgarian Academy of Sciences, 1784 Sofia, Bulgaria

² Institute of Astronomy and Astrophysics, Université Libre de Bruxelles, B-1050 Brussels, Belgium

³ Département de Physique, Université de Montréal, H3C 3J7 Montréal, Québec, Canada

⁴ Institute of Solid State Physics, Bulgarian Academy of Sciences, 1784 Sofia, Bulgaria

E-mail: mutafchieva.y.d@gmail.com

Abstract. Magnetars form a subclass of neutron stars characterized by magnetic fields of order $10^{14} - 10^{15}$ G at their surface. According to numerical simulations, the magnetic fields in their interior could potentially be even stronger. Such magnetic fields are so extreme that the internal constitution of neutron stars may be altered. The effects of Landau-Rabi quantisation of electron motion on the equation of state and on the equilibrium composition of the crust of a neutron star are investigated for a wide range of magnetic field strengths. Both the outer and inner parts of the crust are treated in a unified and consistent way within the nuclear-energy density functional theory.

1. Introduction

Whereas most pulsars are endowed with magnetic fields of order 10^{12} G, some neutron stars may be formed with extremely high magnetic fields of order $10^{14} - 10^{15}$ G, as first proposed by Thompson and Duncan [1]. According to numerical simulations [2–6], the internal magnetic fields can reach $\sim 10^{18}$ G. The existence of such highly magnetised neutron stars so-called magnetars has been confirmed by various astrophysical observations (see, e.g., Ref. [7] for a review).

We have recently shown that the equilibrium properties of the outer and inner crusts of a neutron star could be altered if the magnetic field is strong enough due to Landau-Rabi quantisation of electron motion [8–11]. In this paper, we present new results for intermediate magnetic field strengths.

2. Equilibrium properties of magnetar crusts

2.1. Outer crust

We determine the equilibrium properties of the outer crust of a cold nonaccreted neutron star by minimising the Gibbs free energy per nucleon at each pressure P , as detailed in Ref. [8]. In this model, atoms are supposed to be fully ionised and arranged in a perfect body-centred cubic lattice. We consider only pure layers composed of a single nuclear species with charge number Z and mass number A . Electrons are highly degenerate and are only weakly perturbed by the



Content from this work may be used under the terms of the [Creative Commons Attribution 3.0 licence](https://creativecommons.org/licenses/by/3.0/). Any further distribution of this work must maintain attribution to the author(s) and the title of the work, journal citation and DOI.

ions. For the typical magnetic fields B associated with magnetars, electrons are relativistic since $B_\star \equiv B/B_{\text{rel}} > 1$, where

$$B_{\text{rel}} = \frac{m_e^2 c^3}{e \hbar} \simeq 4.41 \times 10^{13} \text{ G} \quad (1)$$

(m_e is the electron mass, c the speed of light, e the elementary electric charge, and \hbar is the Planck-Dirac constant). The electron motion perpendicular to the magnetic field is quantised into Landau-Rabi orbitals, first calculated by Rabi [12].

Table 1. Composition of the outer crust of a cold nonaccreted magnetar. Results were obtained for a magnetic field strength $B_\star = 500$. Z and A are the charge and mass number of the equilibrium nucleus, \bar{n}_{min} (\bar{n}_{max}) is the minimum (maximum) mean baryon number density at which that nucleus is present and $P_{1 \rightarrow 2}$ is the transition pressure between two adjacent layers. Properties in the upper part of the table are fully determined by experimental atomic masses.

Z	A	\bar{n}_{min} [fm $^{-3}$]	\bar{n}_{max} [fm $^{-3}$]	$P_{1 \rightarrow 2}$ [MeV fm $^{-3}$]
26	56	4.50×10^{-7}	1.36×10^{-6}	1.18×10^{-7}
28	62	1.40×10^{-6}	5.34×10^{-6}	2.95×10^{-6}
28	64	5.51×10^{-6}	7.78×10^{-6}	6.15×10^{-6}
36	86	8.17×10^{-6}	1.25×10^{-5}	1.49×10^{-5}
34	84	1.29×10^{-5}	1.88×10^{-5}	3.23×10^{-5}
32	82	1.95×10^{-5}	2.55×10^{-5}	5.55×10^{-5}
30	80	2.65×10^{-5}	3.29×10^{-5}	8.60×10^{-5}
28	78	3.43×10^{-5}	7.59×10^{-5}	1.40×10^{-4}
28	80	7.78×10^{-5}	8.68×10^{-5}	1.58×10^{-4}
42	124	9.06×10^{-5}	1.22×10^{-4}	2.53×10^{-4}
40	122	1.26×10^{-4}	1.43×10^{-4}	3.20×10^{-4}
39	121	1.45×10^{-4}	1.47×10^{-4}	3.29×10^{-4}
38	120	1.50×10^{-4}	2.07×10^{-4}	4.01×10^{-4}
38	122	2.10×10^{-4}	2.47×10^{-4}	5.07×10^{-4}
38	124	2.51×10^{-4}	2.61×10^{-4}	5.39×10^{-4}

To determine the equilibrium composition of the outer crust, we have made use of the experimental atomic mass data from the 2016 Atomic Mass Evaluation (AME) [13, 14], supplemented by more recent measurements of copper isotopes [15]. For the isotopes for which no experimental data is available, we used the theoretical mass table HFB-24 from the BRUSLIB database [16]. These masses were obtained from self-consistent deformed Hartree-Fock-Bogoliubov calculations with the nuclear energy-density functional BSk24 [17]. Results are collected in tables 1, 2 and 3 for different magnetic field strengths. The outermost layers are made of isotopes with experimentally measured masses. While the stratification of the crust changes with the magnetic field strength, the composition of the deepest layers remains remarkably stable (only the transition pressures and the densities of the different layers are changed).

2.2. Inner crust

Minimising the Gibbs free energy per nucleon at fixed pressure as in the outer crust, is numerically more involved in the inner crust since the pressure now depends on the density of free neutrons in addition to that of electrons. Instead, we have performed the minimisation of

Table 2. Same as Table 1 for $B_\star = 1500$.

Z	A	\bar{n}_{\min} [fm^{-3}]	\bar{n}_{\max} [fm^{-3}]	$P_{1\rightarrow 2}$ [MeV fm^{-3}]
26	56	1.72×10^{-6}	3.86×10^{-6}	2.64×10^{-7}
28	62	4.00×10^{-6}	1.69×10^{-5}	9.71×10^{-6}
28	64	1.75×10^{-5}	1.84×10^{-5}	1.08×10^{-5}
38	88	1.88×10^{-5}	2.44×10^{-5}	1.89×10^{-5}
36	86	2.51×10^{-5}	4.02×10^{-5}	5.07×10^{-5}
34	84	4.16×10^{-5}	5.95×10^{-5}	1.06×10^{-4}
32	82	6.17×10^{-5}	7.96×10^{-5}	1.79×10^{-4}
30	80	8.28×10^{-5}	1.01×10^{-4}	2.70×10^{-4}
46	128	1.06×10^{-4}	1.26×10^{-4}	3.83×10^{-4}
44	126	1.30×10^{-4}	1.37×10^{-4}	4.27×10^{-4}
42	124	1.41×10^{-4}	1.62×10^{-4}	5.66×10^{-4}
40	122	1.68×10^{-4}	1.80×10^{-4}	6.51×10^{-4}
39	121	1.83×10^{-4}	1.84×10^{-4}	6.62×10^{-4}
38	120	1.87×10^{-4}	1.97×10^{-4}	7.33×10^{-4}
38	122	2.00×10^{-4}	2.13×10^{-4}	8.28×10^{-4}
38	124	2.16×10^{-4}	2.20×10^{-4}	8.55×10^{-4}

Table 3. Same as Table 1 for $B_\star = 2500$.

Z	A	\bar{n}_{\min} [fm^{-3}]	\bar{n}_{\max} [fm^{-3}]	$P_{1\rightarrow 2}$ [MeV fm^{-3}]
26	56	3.21×10^{-6}	6.21×10^{-6}	3.56×10^{-7}
28	62	6.46×10^{-6}	2.68×10^{-5}	1.41×10^{-5}
38	88	2.83×10^{-5}	4.33×10^{-5}	3.54×10^{-5}
36	86	4.46×10^{-5}	7.00×10^{-5}	9.14×10^{-5}
34	84	7.23×10^{-5}	1.02×10^{-4}	1.87×10^{-4}
32	82	1.06×10^{-4}	1.29×10^{-4}	2.80×10^{-4}
50	132	1.34×10^{-4}	1.65×10^{-4}	4.30×10^{-4}
46	128	1.74×10^{-4}	2.16×10^{-4}	6.66×10^{-4}
44	126	2.22×10^{-4}	2.34×10^{-4}	7.41×10^{-4}
42	124	2.41×10^{-4}	2.76×10^{-4}	9.76×10^{-4}
40	122	2.85×10^{-4}	3.03×10^{-4}	1.11×10^{-3}
40	124	3.08×10^{-4}	3.13×10^{-4}	1.15×10^{-3}
38	120	3.19×10^{-4}	3.32×10^{-4}	1.24×10^{-3}
38	122	3.37×10^{-4}	3.58×10^{-4}	1.40×10^{-3}
38	124	3.64×10^{-4}	3.70×10^{-4}	1.45×10^{-3}

the Helmholtz free energy at fixed average baryon number density \bar{n} . This latter procedure was shown to be numerically equivalent to the former, the density discontinuities being vanishing small beyond the neutron-drip point [18]. We have obtained the equilibrium properties of the inner crust using the computer code developed by the Brussels-Montreal collaboration [18–

20] and modifying it to take into account the effects of Landau-Rabi quantisation of electron motion. This code is based on the fourth-order extended Thomas-Fermi method with proton shell corrections added perturbatively using the Strutinsky integral theorem. This approach is a computationally very fast approximation to the fully self-consistent Hartree-Fock plus Bardeen-Cooper-Schrieffer method. The Coulomb lattice is described using the Wigner-Seitz approximation. We further assume that electrons are uniformly distributed. Nuclear clusters are supposed to be spherical and their local densities are parametrized as

$$n_q(r) = n_{B,q} + n_{\Lambda,q} \left\{ 1 + \exp \left[\left(\frac{C_q - R_c}{r - R_c} \right)^2 - 1 \right] \exp \left(\frac{r - C_q}{a_q} \right) \right\}^{-1} \quad (2)$$

where $q = p, n$ denotes protons or neutrons respectively and $n_{B,q}$, $n_{\Lambda,q}$, C_q , a_q , and R_c are geometrical parameters of the Wigner-Seitz cell. We only take into account the magnetic-field effects on the electron gas using the analytical approximations implemented in the routines developed by Potekhin and Chabrier [21].

Table 4. Composition of the inner crust of a cold nonaccreted magnetar for different magnetic-field strengths B_\star . Z and N are respectively the mean numbers of protons and neutrons in the Wigner-Seitz cell, \bar{n} is the mean baryon number density of the considered layer.

\bar{n} [fm ⁻³]	$B_\star = 500$		$B_\star = 1500$		$B_\star = 2500$	
	Z	N	Z	N	Z	N
5.474×10^{-4}	40	195	40	211	41	147
9.864×10^{-4}	40	283	41	262	41	271
1.777×10^{-3}	41	426	40	374	40	460
3.203×10^{-3}	40	555	40	548	41	572
5.772×10^{-3}	40	704	40	669	40	624
1.040×10^{-2}	40	824	40	855	40	832
1.874×10^{-2}	40	934	40	965	40	904
3.378×10^{-2}	40	1061	40	1068	40	1044
6.087×10^{-2}	40	1185	40	1193	40	1189

Calculations were carried out using the same generalized Skyrme functional BSk24 [17] as in the outer crust. The influence of the magnetic field on the composition is found to be quite small for the range of magnetic-field strengths considered, as shown in table 4. As in the absence of magnetic fields [22], we find that most layers are still made of clusters with $Z = 40$ and become progressively more neutron rich with increasing density.

The results we obtained for the equation of state over the whole crust region are plotted in figure 1. The effects of the magnetic field lessen with increasing density as electrons fill more and more Landau-Rabi levels. At densities above $\bar{n} \approx 0.01$ fm⁻³ the equation of state matches with that obtained in the absence of magnetic fields. We find that the equation of state remains almost unchanged in the inner crust region for magnetic field strengths below $B_\star = 500$. As can be seen in figure 1, the neutron-drip density delimiting the boundary between the outer and inner crusts does not vary monotonically with B_\star depending on the filling of Landau-Rabi levels (for more details, see [9, 10]).

3. Conclusion

We have determined the equation of state and the composition of the outer and inner crusts of magnetars for different magnetic-field strengths taking into account Landau-Rabi quantisation

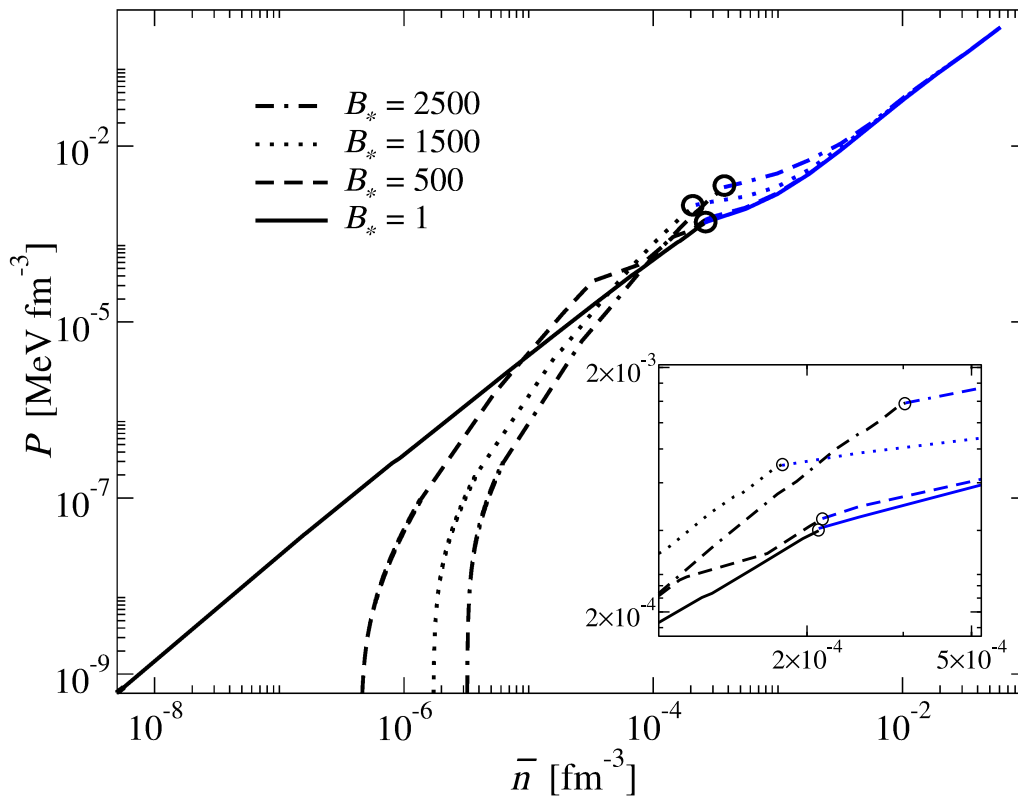


Figure 1. Pressure P in MeV fm^{-3} as a function of the mean baryon number density \bar{n} in fm^{-3} in the outer (black lines) and inner (blue lines) crusts of cold nonaccreted magnetars for different magnetic field strengths B_* . The inset is a close-up view of the neutron-drip transition, marked by the symbol \circ .

of electron motion. Our calculations were carried out in a unified and consistent way within the nuclear-energy density functional theory. The shallowest regions of the crust are found to be the most affected by the magnetic field. At densities above $\approx 0.01 \text{ fm}^{-3}$, the equation of state and the composition appear to be almost unaltered by the magnetic field.

Acknowledgments

This work was financially supported by the National programme “Young scientists” funded by the Bulgarian Ministry of Education and Science, the Bulgarian Science Fund under Contract No.DN08/6, Fonds de la Recherche Scientifique (Belgium), and the “ChETEC” COST Action CA16117 (EU).

References

- [1] Thompson C and Duncan R C 1992 *Astrophys. J.* **392** L9
- [2] Kiuchi K and Yoshida S 2008 *Phys.Rev. D* **78** 044045
- [3] Frieben J and Rezzolla L 2012 *Mon. Not. R. Astron. Soc.* **427** 3406
- [4] Chatterjee D, Elghozi T, Novak J and Oertel M 2015 *Mon. Rot. R. Astron. Soc.* **447** 3785
- [5] Pili A G, Bucciantini N and Del Zanna L 2017 *Mon. Not. R. Astron. Soc.* **470** 2469
- [6] Chatterjee D, Novak J and Oertel M 2019 *Phys. Rev. C* **99** 055811

- [7] Kaspi V and Beloborodov A M 2017 *Ann. Rev. Astron. Astrophys.* **55** 261
- [8] Chamel N, Pavlov R L, Mihailov L M, Velchev C J, Stoyanov Z K, Mutafchieva Y D, Ivanovich M D, Pearson J M and Goriely S 2012 *Phys. Rev. C* **86** 055804
- [9] Chamel N, Stoyanov Z K, Mihailov L M, Mutafchieva Y D, Pavlov R L and Velchev C J 2015 *Phys. Rev. C* **91** 065801
- [10] Chamel N, Mutafchieva Y D, Stoyanov Z K, Mihailov L M and Pavlov R L 2017 *Quantum Systems in Physics, Chemistry, and Biology (Progress in Theoretical Chemistry and Physics no 30)* ed Tadjer A *et al.* (Springer) pp 181–191
- [11] Mutafchieva Y D, Chamel N, Stoyanov Z K, Pearson J M and Mihailov L M 2019 *Phys. Rev. C* **99** 055805
- [12] Rabi I I 1928 *Zeitschrift fur Physik* **49** 507–11
- [13] Huang W J, Audi G, Wang M, Kondev F G, Naimi S and Xu X 2017 *Chin. Phys. C* **41** 030002
- [14] Wang M, Audi G, Kondev F G, Huang W J, Naimi S and Xu X 2017 *Chin. Phys. C* **41** 030003
- [15] Welker A, Althubiti A, Atanasov D, Blaum K *et al.* 2017 *Phys. Rev. Lett.* **119** 192502
- [16] BRUSsels Nuclear LIBrary (BRUSLIB) database <http://www.astro.ulb.ac.be/bruslib/>
- [17] Goriely S, Chamel N and Pearson J M 2013 *Phys. Rev. C* **88** 024308
- [18] Pearson J M, Chamel N, Goriely S and Ducoin C 2012 *Phys. Rev. C* **85** 065803
- [19] Onsi M, Dutta A K, Chatri H, Goriely S, Chamel N and Pearson J M 2008 *Phys. Rev. C* **77** 065805
- [20] Pearson J M, Chamel N, Pastore A and Goriely S 2015 *Phys. Rev. C* **91** 018801
- [21] Potekhin A Y and Chabrier G 2013 *Astron. Astrophys.* **550** A43
- [22] Pearson J M, Chamel N, Potekhin A Y, Fantina A F, Ducoin C, Dutta A K and Goriely S 2018 *Mon. Rot. R. Astron. Soc.* **481** 2994–3026